Influence of asymmetry and nodal planes on high-harmonic generation in heteronuclear molecules

B. B. Augstein and C. Figueira de Morisson Faria

Department of Physics and Astronomy, University College London, Gower Street, London WC1E 6BT, United Kingdom

Abstract. The relation between high-harmonic spectra and the geometry of the molecular orbitals in position and momentum space is investigated. In particular we choose two isoelectronic pairs of homonuclear and heteronuclear molecules, such that the highest occupied molecular orbital of the former exhibit at least one nodal plane. The imprint of such planes is a strong suppression in the harmonic spectra, for particular alignment angles. We are able to identify two distinct types of nodal planes. If the nodal planes are determined by the atomic wavefunctions only, the angle for which the yield is suppressed will remain the same for both types of molecules. In contrast, if they are determined by the linear combination of atomic orbitals at different centers in the molecule, there will be a shift in the angle at which the suppression occurs for the heteronuclear molecules, with regard to their homonuclear counterpart. This shows that, in principle, molecular imaging, which uses the homonuclear molecule as a reference and enables one to observe the wavefunction distortions in its heteronuclear counterpart, is possible.

1. Introduction

High harmonic generation, first discovered in the late 1980s [1], is a process which occurs when atoms or molecules are exposed to intense laser fields, and results in the emission of high frequency coherent radiation. It can be readily understood in terms of the three step model, [2, 3], where an electron is ionized from the atom or molecule, propagates in the laser field, and recombines with its parent ion, upon which high harmonics are released.

Currently, there is much interest in this process due to the possibility of tomographic orbital reconstruction [4, 5, 6], and quantum interference effects [7, 8, 9]. In particular quantum-interference minima and maxima due to high-harmonic emission at spatially separated centers, and high-harmonic suppression due to the presence of nodal planes in the orbital wavefunctions, have been identified and discussed theoretically. Such studies have been extensively performed in diatomic molecules [6, 7, 8, 9, 10, 13, 17]. In many of these studies so far, homonuclear molecules with definite orbital symmetry, either gerade or ungerade, have mostly been used, whereas heteronuclear molecules driven by strong fields are now starting to attract attention [11]. The orbital wavefunctions in such molecules do not have a definite orbital symmetry, and heteronuculear molecules contain a static dipole moment. These attributes will affect the harmonic spectra and other strong field phenomena. Hence, a legitimate question to ask is whether two-center interference patterns in the spectra, or the imprint of nodal planes in form of high-harmonic suppression, can still be observed in the spectra.

In this work, we compare isoelectronic homonuclear and heteronuclear molecules, with particular emphasis on nodal planes in the position space wavefunction and two-center interference effects. We assume the Born-Oppenheimer approximation to be valid, which should hold for large enough molecules [9]. Specifically, we take the pairs Be_2 and LiB, and O_2 and NF. The homonuclear molecule in former and latter pair have a σ_u and π_g highest occupied molecular orbital (HOMO), respectively. Such orbitals contain nodal planes which are altered when a heteronuclear counterpart is chosen. In our investigations, we employ the single-active electron and the strong-field approximation and assume that the HOMO is the only active orbital. The influence of multiple orbitals has been discussed elsewhere [6, 13, 14].

This work is organized as follows. In Sec. 2 the three step model (Sec. 2.1), molecular orbital construction (Sec. 2.2) and interference conditions (Sec. 2.3) are discussed. In Sec. 3, we present our results. This section is split into two main parts. First, in Sec. 3.1, we address the molecular orbitals obtained by us, with a particular emphasis on their nodal planes, or the absence thereof for heteronuclear molecules. Subsequently, in Sec. 3.2 we discuss how such characteristics manifest themselves in the spectra. Finally, in Sec.4 we state the main conclusions to be drawn from this work.

2. Model

2.1. Saddle-point equations

The transition amplitude for high harmonic generation, within the framework of of the strong field approximation (SFA) [2], reads as,

$$b_\Omega = - i \int_{-\infty}^{\infty} dt \int_{-\infty}^{t} dt' \int d^3 k a_{\text{rec}}^*(\mathbf{k} + \mathbf{A}(t)) a_{\text{ion}}(\mathbf{k} + \mathbf{A}(t'))$$
$$\exp[iS(t, t', \Omega, \mathbf{k})] + c.c., \tag{1}$$

with the action

$$S(t, t', \Omega, \mathbf{k}) = -\frac{1}{2} \int_{t'}^{t} [\mathbf{k} + \mathbf{A}(\tau)]^2 d\tau - E_0(t - t') + \Omega t \tag{2}$$

where $a_{\text{rec}}(\mathbf{k} + \mathbf{A}(t)) = \langle \mathbf{k} + \mathbf{A}(t) | \mathbf{d} \cdot \mathbf{e}_x | \Psi \rangle$ and $a_{\text{ion}}(\mathbf{k} + \mathbf{A}(t')) = \langle \mathbf{k} + \mathbf{A}(t') | \mathbf{E}(t') \cdot \mathbf{r} | \Psi \rangle$, are the recombination and ionization prefactors respectively. The terms $\mathbf{d}$, $\mathbf{e}_x$ and Ω denote the dipole operator and the laser-polarization vector and the harmonic frequency, respectively. The ionization potential of the highest occupied molecular orbital, denoted by $|\Psi\rangle$, is given by E_0. The length gauge is used throughout as the interference minima in the harmonic spectra vanish in the velocity gauge [15], and the length form of the dipole operator is used as it accounts for the presence of the static dipole moment ‡.

To solve Eq. (1) we use the saddle-point approximation [16], where the action is stationary, such that $\partial S(t, t', \Omega, \mathbf{k})/\partial t' = \partial S(t, t', \Omega, \mathbf{k})/\partial t = 0$ and $\partial S(t, t', \Omega, \mathbf{k})/\partial \mathbf{k} = \mathbf{0}$. This results in the saddle-point equations

$$\frac{[\mathbf{k} + \mathbf{A}(t')]^2}{2} + E_0 = 0, \tag{3}$$

$$\int_{t'}^{t} d\tau \, [\mathbf{k} + \mathbf{A}(\tau)] = \mathbf{0}. \tag{4}$$

and

$$\frac{[\mathbf{k} + \mathbf{A}(t)]^2}{2} + E_0 = \Omega. \tag{5}$$

These equations have the following physical interpretation. Initially the electron is tunnel ionized from the binding potential. This results in Eq. (3), which gives the conservation of energy. Note that this equation has only complex solutions, as a consequence of the fact that tunneling has no classical counterpart. Secondly, Eq. (4) results in the electron momentum in the continuum being constrained such that the electron returns to its place of origin, which we take to be the geometric center of the molecule. Finally, Eq. (5) represents conservation of energy at recombination.

2.2. Molecular orbitals and dipole matrix elements

The molecular orbitals can be calculated using the Linear Combination of Atomic Orbitals (LCAO) approximation, along with the Born Oppenheimer approximation. Under these assumptions, the molecular orbital wavefunction is given by

$$\Psi(\mathbf{r}) = \sum_\alpha c_\alpha^{(L)} \Phi_\alpha^{(L)}(\mathbf{r} + \mathbf{R}/2)$$
$$+ (-1)^{l_\alpha - m_\alpha + \lambda_\alpha} c_\alpha^{(R)} \Phi_\alpha^{(R)}(\mathbf{r} - \mathbf{R}/2) \tag{6}$$

‡ Recently, we have shown that if a Gaussian basis set is employed in the modeling of the molecular orbitals, the velocity form of the dipole operator leads to a vanishing static dipole moment in heteronuclear molecule. This problem is absent if the length form is taken. For details see [17].

where $\mathbf{R}$ is the internuclear separation, l_α is the orbital quantum number and m_α is the magnetic quantum number. We assume that the ions are positioned along the z axis, i.e., that $\mathbf{R} = R\hat{e}_z$. The coefficients $c_\alpha^{(\xi)}$ form the linear combination of atomic orbitals and are extracted from the quantum chemistry code GAMESS-UK [12]. The indices (L) and (R) refer to the left or to the right ion, respectively, which is a distinction required for heteronuclear molecules, whereas for homonuclear molecules, $c_\alpha^{(L)} = c_\alpha^{(R)} = c_\alpha$ and $\Phi_\alpha^{(R)} = \Phi_\alpha^{(L)} = \Phi_\alpha$. The internuclear axis is taken to be along the z direction, and the laser-field polarization is chosen along the radial coordinate. The parameter λ_α determines the orbital symmetry of the molecular orbital, with $\lambda_\alpha = |m_\alpha|$ and $\lambda_\alpha = |m_\alpha| + 1$ for homonuclear molecules of gerade and ungerade symmetry, respectively.

The wavefunctions themselves are then expanded as Gaussian type orbitals with a real 6-31 basis set, with

$$\Phi_\alpha^{(\xi)}(\mathbf{r}) = \sum_\nu b_\nu^{(\xi)}(r_\chi)^{l_\alpha} e^{-\zeta_\nu^{(\xi)} r^2}. \tag{7}$$

We find that polarized basis sets make little difference to the orbital wavefunctions. For the σ, π_x and π_y orbitals, $r_\chi = z, x$ and y, respectively. The contraction coefficients, $b_\nu^{(\xi)}$ and exponents, $\zeta_\nu^{(\xi)}$, are also obtained from GAMESS-UK [12], while the index ξ distinguishes the left or right ion. Note that these coefficients, along with the coefficients making up the LCAO, are real.

When using the strong-field approximation, all structural information about the molecular orbital is contained in the recombination prefactor, $a_{\rm rec}(\mathbf{k} + \mathbf{A}(t))$, which is given by

$$a_{\rm rec}(\mathbf{k}) = \frac{1}{(2\pi)^{3/2}} \int d^3 r \mathbf{r} \cdot \hat{e}_z \exp[-i\mathbf{k} \cdot \mathbf{r}] \Psi(\mathbf{r}). \tag{8}$$

This is the component of $i\partial_{\mathbf{k}}\Psi(\mathbf{k})$ along the laser-field polarization. This prefactor gives rise to any two center interference which occurs in the harmonic spectra. The ionization prefactor, $a_{\rm ion}(\mathbf{k} + \mathbf{A}(t'))$, on the other hand, will mainly determine whether tunnel ionization will be suppressed or enhanced due to the shape of a particular orbital. Therefore it directly affects the overall harmonic yield, but is not responsible for any interference patterns. Both prefactors are vanishing for nodes in the molecular orbitals.

In this work we use the momentum space wavefunctions to calculate the prefactors, which are given by

$$\psi(\mathbf{k}) = \sum_\alpha \exp[i\mathbf{k}\cdot\frac{\mathbf{R}}{2}] c_\alpha^{(L)} \Phi_\alpha^{(L)}(\mathbf{k}) \tag{9}$$

$$+ (-1)^{l_\alpha - m_\alpha + \lambda_\alpha} \exp[-i\mathbf{k}\cdot\frac{\mathbf{R}}{2}] c_\alpha^{(R)} \Phi_\alpha^{(R)}(\mathbf{k}),$$

where

$$\Phi_\alpha^{(\xi)}(\mathbf{k}) = \sum_\nu b_\nu^{(\xi)} \tilde{\varphi}_\nu^{(\xi)}(\mathbf{k}), \tag{10}$$

with

$$\tilde{\varphi}_\nu^{(\xi)}(\mathbf{k}) = (-ik_\beta)^{l_\alpha} \frac{\pi^{3/2}}{2^{l_\alpha} \left(\zeta_\nu^{(\xi)}\right)^{3/2 + l_\alpha}} \exp[-k^2/(4\zeta_\nu^{(\xi)})]. \tag{11}$$

Similarly to the position space expressions, $\beta = z$, $\beta = x$ and $\beta = y$ for the σ, π_x and π_y orbitals. The return condition (4) guarantees that the momentum $\mathbf{k}$ and the external field are collinear. Hence, for a linearly polarized field the angle between the intermediate momentum $\mathbf{k}$ and the internuclear axis $\mathbf{R}$ is equal to the alignment angle θ_L between the molecule and the field. The above-stated equations have been derived under the assumption that only s and p states will be employed in order to build the wavefunctions utilized in this work. For more general expressions see Ref. [13].

2.3. Interference Condition

Maxima and minima in the momentum-space wavefunction may be determined by writing the exponents in Eq. (10) in terms of trigonometric functions. In this case, one obtains

$$\psi(\mathbf{k}) = \sum_\alpha \mathcal{C}_+^{(\alpha)} \cos\left[\frac{\mathbf{k} \cdot \mathbf{R}}{2}\right] + i\mathcal{C}_-^{(\alpha)} \sin\left[\frac{\mathbf{k} \cdot \mathbf{R}}{2}\right], \tag{12}$$

with

$$\mathcal{C}_\pm^{(\alpha)} = (-1)^{l_\alpha - m_\alpha + \lambda_\alpha} c_\alpha^{(R)} \Phi_\alpha^{(R)}(\mathbf{k}) \pm c_\alpha^{(L)} \Phi_\alpha^{(L)}(\mathbf{k}). \tag{13}$$

Calling $\vartheta = \arctan[i\mathcal{C}_+^{(\alpha)}/\mathcal{C}_-^{(\alpha)}]$,we find

$$\psi(\mathbf{k}) = \sum_\alpha \sqrt{\left(\mathcal{C}_+^{(\alpha)}\right)^2 - \left(\mathcal{C}_-^{(\alpha)}\right)^2} \sin[\vartheta + \mathbf{k} \cdot \mathbf{R}/2]. \tag{14}$$

Eq. (14) exhibit minima for $\vartheta + \mathbf{k} \cdot \mathbf{R}/2 = n\pi$.

Note, however, that the coefficients $\mathcal{C}_\pm^{(\alpha)}$ defined in Eq. (13) depend on the wavefunctions at the left and right ions. Since these wavefunctions themselves depend on the momentum $\mathbf{k}$, one expects the two-center patterns to be blurred for heteronuclear molecules. In contrast, for homonuclear molecules, $c_\alpha^{(L)} = c_\alpha^{(R)}$ and $\Phi_\alpha^{(L)}(\mathbf{k}) = \Phi_\alpha^{(R)}(\mathbf{k})$. This implies that the momentum dependence in the argument ϑ cancels out and that the interference condition in Refs. [8, 13] is recovered. In this case, sharp interference fringes are expected to be present.

The above-stated condition does not only lead to interference fringes in the bound-state momentum wavefunctions but also in the high-harmonic spectra. This is due to the fact that the dipole matrix elements depend on the wavefunctions (10). In this latter case, $\mathbf{k} \to \mathbf{k} + \mathbf{A}(t)$ in Eqs. (10)-(14).

For a linearly polarized monochromatic field of frequency ω, using the saddle-point equation (5), the generalized interference condition (14) may be expressed in terms of the harmonic order n as

$$n = \frac{E_0}{\omega} + \frac{2(\kappa\pi - \vartheta)^2}{\omega R^2 \cos^2\theta_L}, \tag{15}$$

where E_0 is the absolute value of the bound-state energy in question, κ is an integer number, θ_L is the alignment angle, R is the internuclear distance and ϑ is defined above). This interference condition has been first derived in [18] and has been used by us in previous work [13].

In the specific case of orbitals of π_g type, which are constructed entirely from p-type atomic orbitals such that $l_\alpha = 1$, are of gerade symmetry such that $\lambda_\alpha = 0$, and are made from a homonuclear species such that $\Phi_\alpha^{(R)}(\mathbf{k}) = \Phi_\alpha^{(L)}(\mathbf{k})$ and $c_\alpha^{(R)} = c_\alpha^{(L)}$,
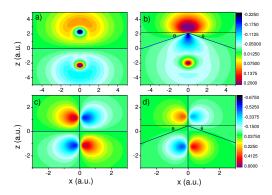
Figure 1. Highest occupied molecular orbitals in position space for the homonuclear molecules Be_2 and O_2 [panels a) and c)], and their heteronuclear isoelectronic counterparts LiB and NF [panels b) and d)]. The orbital symmetries in panels a), b), c) and d) are $2\sigma_u$, 4σ, $1\pi_g$ and 2π, respectively, and the bond lengths are $R^{(Be_2)} = 4.642$ a.u., $R^{(LiB)} = 4.642$ a.u., $R^{(O_2)} = 2.280$ a.u., and $R^{(NF)} = 2.485$ a.u.

one finds that $\vartheta = 0$. This implies that for the zeroth order interference, where $\kappa = 0$, the second term of (15) will vanish leaving the angular independent term

$$n = \frac{E_0}{\omega}. \tag{16}$$

This minimum, however, would occur exactly at the ionization threshold, for which the present framework is expected to break down. Hence, it will not be discussed here.

3. Results

3.1. Position and momentum space wavefunctions

In this section, we will display the specific molecular orbitals employed by us in the results that follow. We choose two pairs of molecules composed of a homonuclear molecule and an isoelectronic heteronuclear molecule. The first pair, Be_2 and LiB, possess eight electrons and a σ highest occupied molecular orbital, while the second pair, O_2 and NF, have sixteen electrons and a π highest occupied molecular orbital.

In Fig. 1, we exhibit the HOMO for homonuclear molecules, Be_2 and O_2, and heteronuclear molecules, LiB and NF, as obtained with GAMESS-UK [Figs. 1.(a),(b),(c) and (d) respectively]. The internuclear axis is aligned along the z-axis. The position-space wavefunctions of Be_2 and LiB are of σ type with Be_2 having ungerade symmetry, σ_u, and a nodal plane along the x-axis at $z = 0$. For LiB, there is a bias towards the Boron atom. One can also clearly see the contribution of the p type atomic orbital which is introduced by the Boron atom. The position-space wavefunctions of O_2 and NF are of π type with O_2 having gerade symmetry, π_g, and a nodal plane along the x-axis at $z = 0$ and the z-axis at $x = 0$. NF shows a bias towards the Fluorine atom.

We have found that both momentum-space wavefunctions, given in Figs. 2, 3 and 4, are symmetric with respect to $(p_x, p_z) \rightarrow (-p_x, -p_z)$ in comparison to their
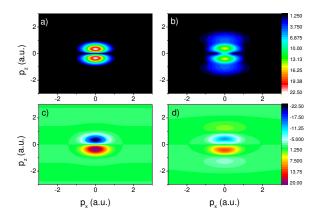
Figure 2. Absolute values and imaginary parts of the highest occupied molecular orbitals in momentum space for the homonuclear molecule Be_2 [panels a) and c) respectively] and its heteronuclear counterpart LiB [panels b) and d)].

position-space counterparts. Despite that, the momentum-space wavefunctions for homonuclear and heteronuclear molecules exhibit different properties, especially if a real basis set is used in the construction of the position-space wavefunctions $\psi(\mathbf{r})$. They come from the properties of Fourier transforms and will determine whether a particular node will be blurred in the heteronuclear case. An even wavefunction in position space will lead to a real wavefunction in momentum space, as the Fourier transform of a real and even function should be real. For the same reason, if the position-space wavefunction is odd, the corresponding momentum-space wavefunction should be pure imaginary. Neither property will hold if the position-space wavefunction does not possess a well-defined symmetry. In this case, its momentum-space counterpart will be complex.

We will now have a closer look at the nodes in the momentum-space wavefunctions. For Be_2, the momentum-space wavefunction of the σ_u HOMO is pure imaginary, and exhibit a clear node along the p_x-axis (see Figs. 2.(a) and (c) for $|\psi(\mathbf{k})|$ and $\text{Im}[\psi(\mathbf{k})$, respectively). This node is caused by the linear combination of atomic orbitals giving rise to the σ_u orbital.

The above-mentioned node is lost in the absolute value of the HOMO wavefunction of LiB, shown in Fig. 2.(b), even though a suppression along the p_x axis is still present. Apart from that, there is a secondary set of peaks extending towards higher momentum values. One should note, however, that a very clear central node for LiB at the p_x axis can be seen in the imaginary part of corresponding wavefunction, shown in Fig. 2.(d). This feature is blurred by the real part of $\psi(\mathbf{k})$, which does not have this node, and is of comparable magnitude (see Fig. 4.(a)). As discussed above, a complex wavefunction in momentum space is related to an asymmetric wavefunction in position space. Hence, the loss of symmetry in position space is what leads to the loss of the clear nodal plane in momentum space. Physically, the asymmetry in the position-space wavefunction can be traced back to the static dipole moment along the internuclear axis.
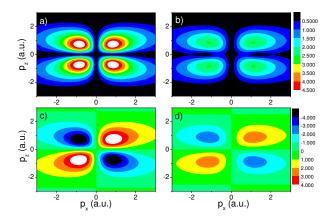
Figure 3. Absolute values and real parts of the highest occupied molecular orbitals in momentum space for homonuclear molecule O_2 [panels a) and c) respectively] and its heteronuclear counterpart NF [panels b) and d)].
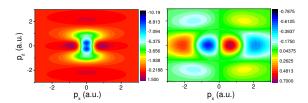

Figure 4. Real part of the highest occupied molecular orbital in momentum space for LiB and imaginary part of the highest occupied molecular orbital in momentum space for NF, panels a) and b) respectively.

In comparing O_2 and NF momentum space wavefunctions as shown in Fig. 3, one can see that the features are quite similar for one of the nodal planes. Specifically, the well defined nodal plane along the p_x-axis observed for O_2 has been slightly blurred for NF (see Figs. 3.(a) and (b), respectively). This again is because of the loss of symmetry in the heteronuclear case, due to the static dipole moment. Note once more that an even and real position-space wavefunction, such as the HOMO in O_2, leads to a real momentum-space wavefunction. This is not the case for NF, and the non-vanishing imaginary part of the momentum space wavefunction gives rise to the blurring. However, it can be seen from Fig. 4.(b) that the imaginary part of the momentum space wavefunction for NF is much smaller than its real part. This implies that the NF molecule is quite close to having gerade type symmetry, and therefore one would expect similar features in the position and momentum space wavefunctions as compared to O_2.

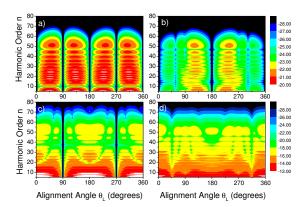In contrast, the other nodal plane, along the z-axis, remains completely unaffected

Figure 5. Harmonic spectra as a function of alignment angle for the molecule a) Be_2 of ionization potential 0.2390 a.u., b) LiB of ionization potential 0.1942 a.u., c) O_2 of ionization potential 0.2446 a.u. and d) NF of ionization potential 0.2246 a.u. A linearly polarized laser field of frequency ω=0.057 a.u. and intensity $I = 4 \times 10^{14}$W/cm^2 is used. The spectra have been computed using the length gauge and employing the dipole operator in the length form.

by the presence of the static dipole moment. Indeed, this nodal plane is just as pronounced in both molecules, irrespective of being homonuclear or heteronuclear. Mathematically, this is because one can define two types of nodal planes in position space: one of which is due to the characteristic of the p-type atomic orbitals, which are of the form $\sum_\nu b_\nu^{(\xi)} x e^{-\zeta_\nu^{(\xi)} r^2}$, and therefore disappear at $x = 0$, irrespective of the contraction coefficients and exponential coefficients, and the other of which is due to the linear combination of atomic orbitals. The latter results in a cancelation for a homonuclear molecule, and hence a nodal plane. This however does not occur for a heteronuclear molecule. The nodal plane along the p_z-axis is of the first type, and is therefore present for both molecules, and the nodal plane along the p_x-axis is of the second type and not present for NF. This argument can be mapped into the momentum space using Fourier transforms (see Eq. (10)).

3.2. Harmonic Spectra

We now present the harmonic spectra computed in a linearly polarized monochromatic wave of frequency ω and amplitude ωA_0, for all molecules discussed previously. These results are displayed in Fig. 5. It can be seen that all spectra contains a series of cuts, i.e., a complete suppression of the yield for particular angles. Most notably in the case of O_2 these occur at alignment angles θ_L=0,90,180,270 and 360 degrees (see Fig. 5.(a)). By observing the position space wavefunction in Fig. 1.(c) and the absolute value of the momentum space wavefunction in Fig. 3.(a) this can immediately

be attributed to the nodal planes of the molecular wavefunction, which occur at these angles, and therefore prohibit ionization or recombination. The situation in the case of NF , however, is modified, as shown in Fig. 5.(b). The harmonic signal completely vanishes at alignment angles θ_L=0,180 and 360 degrees, because at these angles the nodal planes in the highest occupied molecular orbital occur due to the nature of the p-type atomic orbitals. However, due to the polar nature of these heteronuclear molecules, and a linear combination of atomic orbitals which no longer cancels out, the nodal planes at alignment angles θ_L=90 and 270 degrees are no longer present.

In fact, several differences with regard to the homonuclear case are observed. Firstly, the signal is no longer completely suppressed, but there is a distinct minimum which occurs at alignment angles θ_L= 54 and 306 degrees. There is also a second minimum, but not a cut, beyond harmonic n=35, which occurs at the alignment angles θ_L=90 and 270 degrees, that is, where the nodes were in the homonuclear molecule. We attribute this to the remnants of the nodal plane in its heteronuclear counterpart. This can be seen more clearly in Fig. 7.(a), where the harmonic spectra of O_2 and NF are plotted as functions of the alignment angle for fixed harmonic order.
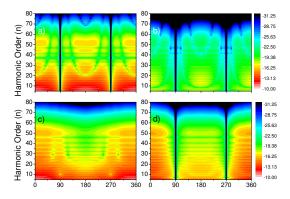
Inspection of the position and momentum space wavefunction suggests that the polar nature of the heteronuclear molecules deforms the nodal plane such that, although there is no longer a node, there is a suppression which occurs at the angle to which the plane has been deformed. As the molecule is rotated the new minimum in the wavefunction is first experienced before θ_L=90 degrees but then occurs at the same angle after θ_L=270 degrees. Therefore the spectra has reflectional symmetry about an alignment angle of 180 degrees. There is no longer a clear nodal plane, as the probability density associated to the wavefunction is small, but nonvanishing. Hence, there is not a complete suppression in the harmonic spectra. However, a clear minimum is still visible.

Note that, for O_2, the two-center interference maxima and minima predicted by Eq. (16) are located either beyond the cutoff or at the ionization threshold. Therefore, they do not occur in the parameter range of interest. This also holds for its heteronuclear counterpart.

Now observing the spectra for Be_2, displayed in Fig. 5.(c), one may identify nodes at θ_L=90 and 270 degrees, as one would expect by observing the position and momentum space wavefunctions. In the spectra of the heteronuclear counterpart LiB, presented in Fig. 5.(d), these nodes have been replaced by minima at θ_L=45 and 315 degrees, for the same reasons as described above.

The spectra for Be_2 also exhibit two-center interference minima, corresponding to $\kappa = 0$, $\kappa = 1$ and $\kappa = 2$ in Eq. (15), whose energy position depends strongly on the alignment angle. These are shifted considerably in the heteronuclear counterpart LiB. This is because the Be_2 molecular wavefunction is constructed almost entirely of s-type atomic orbitals, whereas in the case of LiB the Boron atom introduces p-type atomic orbitals into the molecular wavefunction and hence changes the interference condition. Note that, with regard to Be_2, there is a blurring in the two-center patterns for LiB. This is expected according to the discussion in Sec. 2.3.

This is shown in more detail in Fig. 6, in which the individual contributions of the s and p states to the spectra of Be_2 and LiB are presented (upper and lower panels, respectively). For these individual contributions, there is also a considerably simpler interference condition for homonuclear molecules, which can be obtained from Eq. (15) by setting either C_+ or C_- equal to zero. Specifically the s-state and p-state

Figure 6. Harmonic spectra as a function of alignment angle for a) the s-type orbitals of the Be_2 HOMO, b) the p-type orbitals of the Be_2 HOMO, c) the s-type orbitals of the LiB HOMO, d) the p-type orbitals of the LiB HOMO, for the same parameters as in the previous figure.

contributions for an ungerade orbital exhibit minima at the harmonic frequencies

$$\Omega_s^{(u)} = E_0 + \frac{2\kappa^2\pi^2}{R^2\cos^2\theta_L} \tag{17}$$

and

$$\Omega_p^{(u)} = E_0 + \frac{(2\kappa+1)^2\pi^2}{2R^2\cos^2\theta_L}, \tag{18}$$

respectively, where κ is a integer. In Fig. 6.(a), we may identify the minima for $\kappa = 1$ and $\kappa = 2$ according to Eq. (17), while in Fig. 6.(b) the minima corresponding to $\kappa = 0$ and $\kappa = 1$ can be easily found. If the s p mixing is considered, the full expression (15) must be used.

The contributions from p-type orbitals to the harmonic spectrum of Be_2 are orders of magnitude smaller than the contribution of p-type orbitals in LiB. Therefore the overall spectrum of Be_2 is dominated mostly by the s-type atomic orbitals. In contrast, in LiB, both types of orbitals lead to comparable contributions to the spectra, and the s p mixing will influence the energy position of the overall two-center patterns. Apart from that, the ionization potentials and internuclear separation of both molecules are slightly different. This will influence the two-center interference further.

The effects of s p mixing are also displayed in Fig. 7.(b) and Fig. 7.(c) for a fixed mid-plateau harmonic. The figure clearly shows that where one observes that, for Be_2, the s-type orbitals dominate and the main effect of the p-type orbitals is to introduce a small shift in the interference minima. On the other hand, for LiB, the overall maxima and minima are considerably altered by s p mixing. In the figure, one can also see that the nodal planes occurring at alignment angles θ_L=90 and 270 degrees in Be_2, are shifted by the contribution of the s-type orbitals in LiB.

Finally, we will comment on the overall harmonic intensities. The harmonics generated from NF are less intense than those from O_2. As the ionization potential of
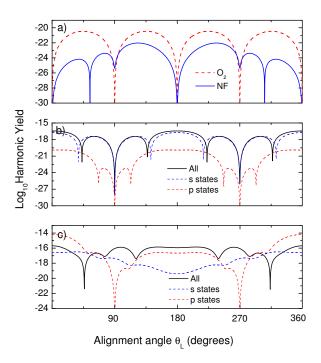
Figure 7. The harmonic yield of a) O_2 and NF for the 45th harmonic vs the alignment angle, b) s and p orbitals to the harmonic yield of Be_2 for the 25th harmonic vs the alignment angle and c) s and p orbitals to the harmonic yield of LiB for the 25th harmonic vs the alignment angle. All parameters are the same as in the previous figure.

NF is slightly lower than that of O_2, one would expect more ionization and therefore higher harmonic yield. This implies that the shape of the molecular wavefunction results in suppression at the recombination step for NF, an effect which is more prominent than the difference in ionization potential. Harmonics generated from Be_2 and LiB are much more intense than those generated by O_2 and NF, despite similar ionization potentials. This suggests that the presence of nodal planes, or minima associated with strong suppression of the wave function, reduce the yield of the entire spectrum. As O_2 has two nodal planes and Be_2 has one, harmonic spectra from the former is less intense than that of the latter.

4. Conclusions

In this work, we investigated the dependence of the high-order harmonic spectra on the alignment angle between the diatomic molecules and the laser-field polarization, for isoelectronic pairs consisting of a homonuclear and a heteronuclear molecule. We employed a single active electron approximation, using the HOMO as the active orbital, within the strong-field approximation.

Our studies lead us to conclude that there are two types of nodes in the bound-

state orbitals of molecules, which will lead to a strong suppression in the harmonic yield when such nodes are parallel to the laser–field polarization. The first type is caused by the nodes in the atomic orbitals at *each* ion, and is present at the same location for homonuclear molecules and their heteronuclear counterparts. The second type of node is due to the sum or subtraction of atomic orbitals at *different* centers within the linear combination of atomic orbital (LCAO) approximation. Both types of minima are present for homonuclear molecules. For their heteronuclear counterparts, however, the asymmetry of the molecule eliminates the latter nodes. This implies that the imprints of the first type of nodes in the harmonic spectra are common to isoelectronic homonuclear and heteronuclear molecules, and could in principle be observed in both cases.

In general, the asymmetry also leads to some blurring in the interference patterns caused by high-harmonic emission at spatially separated centers in the molecule. Furthermore, depending on the molecule, $s\,p$ mixing will be different. This will lead to shifts in the energy positions of the two-center patterns. On a more technical level, we have also been able to map the symmetry or asymmetry of the molecular orbitals in position space to properties of their momentum-space counterparts.

The above-stated findings show that nodal planes in a heteronuclear molecule can be related to those in an isoelectronic homonuclear molecule. Hence, in principle, the latter can be used as a reference point in order to understand the behavior of the former, by using high-order harmonic generation. The shifts in the nodal planes due to the distortions in the wavefunctions or the absence thereof can be mapped into features in the high-harmonic spectra. This may shed some light in the imaging of heteronuclear molecules.

Acknowledgments

[1] McPherson A, Gibson G, Jara H, Johann U, Luk T S, McIntyre I A, Boyer K, and Rhodes C K 1987 *J. Opt. Soc. Am. B* **4**, 595.
[2] Lewenstein M, Balcou Ph, Ivanov M Yu, L'Huillier A and Corkum P B 1994 *Phys. Rev. A* **49**, 2117.
[3] Corkum P B 1993 *Phys. Rev. Lett.* **71**, 1994.
[4] Kanai T, Minemoto S and Sakai H 2005 *Nature* **435**, 470.
[5] Itatani J, Levesque J, Zeidler D, Niikura H, Pépin H, Kieffer J C, Corkum P B and Villeneuve D M 2004 *Nature* **432**, 867.
[6] Smirnova O, Mairesse Y, Patchkovskii S, Dudovich N, Villeneuve D, Corkum P B, Ivanov M Y 2009 *Nature* **460**, 972.
[7] Lein M, Hay N, Velotta R, Marangos J P, and Knight P L 2002 *Phys. Rev. Lett.* **88**, 183903; 2002 *Phys. Rev. A* **66**, 023805; Spanner M, Smirnova O, Corkum P B and Ivanov M Y 2004 *J. Phys. B* **37**, L243.
[8] Milošević D B 2006 *Phys. Rev. A* **74**, 063404; Busuladžić M, Gazibegović-BusuladžićA, Milošević D B, and Becker W 2008 *Phys. Rev. Lett.* **100**, 203003; 2008 *Phys. Rev. A* **78**, 033412.
[9] Madsen C B and Madsen L B, 2006 *Phys. Rev. A* **74**, 023403; Madsen C B, Mouritzen A S, Kjeldsen T K, and Madsen L B, 2007 *Phys. Rev. A* **76**, 035401.
[10] Chu X and Chu S I, 2001 *Phys. Rev. A* **64**, 063404; Telnov D A and Chu S- I 2009, *Phys. Rev. A* **80**, 043412; Chu X and Chu S I; 2004 *Phys. Rev. A* **70**, 061402; Son S -K and Chu S I 2009 *Phys. Rev. A* **80**, 011403.
[11] Holmegaard L, Hansen J L, Kalhj L, Kragh S L, Stapelfeldt H, Filsinger F, Kpper J, Meijer G, Dimitrovski D, Abu-samha M, Martiny C P J, and Madsen L B 2010 *Nature Phys.* **6**, 428; Etches A and Madsen L B 2010 *J. Phys. B* **43**, 155602.

[12] GAMESS-UK is a package of ab initio programs. See: "http://www.cfs.dl.ac.uk/gamess-uk/index.shtml", Guest M F, Bush I J, van Dam H J J, Sherwood P, Thomas J H, van Lenthe J H, Havenith R W A, Kendrick J 2005 *Mol. Phys.* **103**, 719.

[13] Figueira de Morisson Faria C and Augstein B B 2010 *Phys. Rev. A* **81**, 043409.

[14] Patchkovskii S, Zhao Z, Brabec T and Villeneuve D M 2006 *Phys. Rev. Lett.* **97**, 123003; Patchkovskii S, Zhao Z, Brabec T, and Villeneuve D M, 2007 *J. Chem. Phys.* **126**, 114306; Smirnova O, Patchkovskii S, Mairesse Y, Dudovich N, Villeneuve D, Corkum P B, and Ivanov M Yu 2009 *Phys. Rev. Lett.* **102**, 063601.

[15] Figueira de Morisson Faria C 2007 *Phys. Rev. A* **76**, 043407; Smirnova O, Spanner M and Ivanov M, 2007 *J. Mod. Opt.* **54**, 1019.

[16] Figueira de Morisson Faria C, Schomerus H and Becker W 2002 *Phys. Rev. A* **66**, 043413.

[17] Augstein B B and Figueira de Morisson Faria C, arXiv: 1007.2135 [atom.ph]

[18] Odžak S and Milošević D B 2009 *Phys. Rev. A* **79**, 023414; 2009 *J. Phys. B* **42**, 071001.